Starship giant transposable elements cluster by host taxonomy using kmer-based phylogenetics

Rowena Hill[1,*], Daniel Smith[2,†], Gail Canning[3], Michelle Grey[1], Kim E. Hammond-Kosack[3,*], Mark McMullan[1,*]

[1]Earlham Institute, Norwich, Norfolk, NR4 7UZ, UK

[2]Intelligent Data Ecosystems, Rothamsted Research, Harpenden, Hertfordshire, AL5 2JQ, UK

[3]Protecting Crops and the Environment, Rothamsted Research, Harpenden, Hertfordshire, AL5 2JQ, UK

[†]Present address: Department of Computational and Systems Biology, John Innes Centre, Norwich, Norfolk, NR4 7UH, UK

*Corresponding authors: Rowena.Hill@earlham.ac.uk (R.H.); kim.hammond-kosack@rothamsted.ac.uk (K.H-K.); Mark.McMullan@earlham.ac.uk (M.M.)

Running head: Kmer-based phylogenetics of *Starships*

ABSTRACT

Starships are a recently established superfamily of giant cargo-mobilising transposable elements in the fungal subphylum *Pezizomyotina* (phylum *Ascomycota*). To date, *Starship* elements have been identified up to ~700 Kbp in length and carrying hundreds of accessory genes, which can confer both beneficial and deleterious traits to the host genome. Classification of *Starship* elements is centred on the tyrosine recombinase gene that mobilises the element, termed the captain. We contribute a new perspective to *Starship* relatedness by using an alignment-free kmer-based phylogenetic tree building method, which can infer relationships between elements in their entirety, including both active and degraded elements and irrespective of high variability in element length and cargo content. In doing so we found that relationships between entire *Starships* differed from those inferred from captain genes and revealed patterns of element relatedness corresponding to host taxonomy. Using *Starships* from root/soil-dwelling *Gaeumannomyces* species as a case study, we found that kmer-based relationships correspond with similarity of cargo gene content. Our results provide insights into the prevalence of *Starship*-mediated horizontal transfer events. This novel application of a kmer-based phylogenetics approach overcomes the issue of how to represent and compare highly variable *Starship* elements as a whole, and in effect shifts the perspective from a captain to a cargo-centred concept of *Starship* identity.

Keywords: cargo-mobilising elements, *Gaeumannomyces*, *Ascomycota*, *Pezizomycotina, Fungi*

INTRODUCTION

Transposable elements (TEs), or transposons, are stretches of DNA, typically between 100 to 10,000 bp in length, which can independently move and replicate within the genome (Biémont 2010; Wells and Feschotte 2020). Thanks to advances in long-read sequencing, highly contiguous genome assemblies have revealed the existence of TEs hundreds of kilobases in length (Arkhipova and Yushenova 2019). Some of these large TEs have been shown to harbour both genes necessary for their mobilisation as well as miscellaneous accessory genes, and are accordingly referred to as cargo-mobilising elements (CMEs; Gluck-Thaler and Vogan 2024). Recently, giant CMEs have been found in various species in the fungal subphylum *Pezizomycotina* (phylum *Ascomycota*; McDonald et al. 2019; Vogan et al. 2021; Urquhart et al. 2022), and have since been determined to belong to a newly established TE 'superfamily' (*sensu* Wicker *et al.* (2007)) or 'subclass' (*sensu* Wells and

Feschotte (2020)) known as '*Starships*' (Gluck-Thaler *et al.* 2022). To date, *Starship* CMEs have been found to range in length from 15 Kbp (Gluck-Thaler *et al.* 2024) to ~700 Kbp (Urquhart *et al.* 2024).

Starship mobilisation is mediated by a leading 5' located gene containing the DUF3435 domain (protein family accession PF11917), termed the 'captain', which encodes a tyrosine recombinase that initiates movement of the TE into a new genomic location via a 'cut-and-paste' mechanism (Urquhart *et al.* 2023). This is similar to the hypothesised mobilisation process of the '*Crypton*' Class II DNA transposon superfamily (Wells and Feschotte 2020), which was incidentally also first discovered in fungi (Goodwin *et al.* 2003), although this TE superfamily has since been found in other eukaryotes (Kojima and Jurka 2011). Tyrosine recombinase domains in *Starship* captain genes and *Cryptons* are very distantly related (Gluck-Thaler *et al.* 2022) and, unlike *Cryptons*, *Starship* elements are sometimes flanked by tandem inverted repeats (TIRs) in addition to direct repeats (DRs), and can contain a highly variable and often sizeable cargo of accessory genes (Gluck-Thaler and Vogan 2024). *Starship* cargos can harbour genes that are beneficial to the fungus, for example those associated with plant virulence (McDonald *et al.* 2019), metal tolerance (Urquhart *et al.* 2022) and climate adaptation (Tralamazza *et al.* 2024). However, as selfish genetic elements, *Starships* may also mobilise cargo which is neutral or even detrimental to the overall fitness of the host genome (Vogan *et al.* 2021).

Classification within the *Starship* CME superfamily is focused on the captain gene, using both phylogenetic relationships between captain genes to define 'family' and orthologue clustering of captain genes to define 'navis' (i.e. a ship) (Gluck-Thaler and Vogan 2024). Both the captain family and the flanking DRs are thought to influence the genomic site that an element is inserted into, with *Starships* of certain captain families preferentially inserting into, for instance, other TEs or 5S rDNA (Urquhart *et al.* 2023; Gluck-Thaler and Vogan 2024). DUF3435-containing tyrosine recombinase genes are more usually found 'solo', rather than within a cargo-carrying element i.e. as a captain, however it is not clear to what extent this is due to the failure to detect the boundaries of an element or because pseudogenisation of the tyrosine recombinase gene has occurred (Gluck-Thaler and Vogan 2024). *Starship* captain genes do not form a single monophyletic cluster in the DUF3435 tyrosine recombinase gene tree, and are instead scattered across the phylogeny amongst other apparently 'solo' DUF3435-containing tyrosine recombinase genes (Gluck-Thaler *et al.* 2022; Hill *et al.* 2025). Due to their highly divergent nature, tyrosine recombinase gene sequences are also difficult to align, introducing uncertainty into conventional alignment-based phylogenetic analyses.

It is not currently possible to determine whether these relationships described by captains are preserved or representative of the *Starships* as a whole, considering that elements are highly variable in terms of cargo and overall length. This also limits phylogenetic assessment of the prevalence of (or boundaries to) horizontal exchange across the *Pezizomycotina*. In an effort to represent distinction in cargo content, Gluck-Thaler and Vogan (2024) introduced the additional definition of 'haplotype', based on clustering of kmer similarity scores. Here, we have taken this approach one step further and used a kmer-based phylogenetic tree building method to contribute a new perspective to *Starship* relatedness. In doing so we have revealed previously obscured patterns of *Starship* relatedness corresponding to host taxonomy.

To determine whether the relatedness revealed by the kmer trees conformed with similarity in cargo gene content, we explored the cargos of *Starships* previously identified from genomes within the genus *Gaeumannomyces* (Hill *et al*. 2025). This genus comprises soil-dwelling fungi which are also both pathogenic and non-pathogenic wheat and wild grass root associates (Palma-Guerrero *et al*. 2021; Chancellor *et al*. 2024). These elements provided an ideal case-study as they vary greatly in overall size and number of cargo genes within their host-taxonomy clusters. The genomes were also all generated in parallel using the same long-read sequencing technology and a cross-referent annotation pipeline (Hill *et al*. 2025). Given the impact of assembly and annotation quality on *Starship* recovery (Gluck-Thaler and Vogan 2024), these *Gaeumannomyces* elements therefore represent a consistent dataset that are impacted to a lesser extent by the technology used to produce them.

MATERIALS AND METHODS

Kmer-based phylogenetic analysis

To compare phylogenetic reconstruction of whole elements versus captain genes, we used a curated set of 39 *Starships* from Gluck-Thaler *et al*. (2022) and Gluck-Thaler and Vogan (2024) alongside 14 *Gaeumannomyces Starships* predicted using the tool starfish v1.0.0 (Gluck-Thaler and Vogan 2024) in our previous study (Hill *et al*. 2025). Only *Gaeumannomyces Starships* with predicted flanking repeats were used. We used entire element sequences as input for the kmer-based method Mashtree v1.4.6 (Katz *et al*. 2019) with 1,000 bootstrap replicates and the --min-depth 0 parameter to discard very unique kmers, recommended to improve accuracy. We used the

corresponding captain genes as input for a maximum likelihood (ML) tree, first aligning gene sequences using MAFFT v7.271 (Katoh and Standley 2013), trimming using trimAl v1.4.rev15 (Capella-Gutiérrez *et al*. 2009), and finally building the ML tree using RAxML-NG v1.1.0 (Kozlov *et al*. 2019) with bootstrapping until convergence, which occurred after 150 bootstrap replicates. We visualised concordance between the two phylogenies via a tanglegram, produced in R v4.3.1 (R Core Team 2023) using the packages ape v5.7-1 (Paradis and Schliep 2019), phytools v2.1-1 (Revell 2024) and ggtree v3.9.1 (Yu *et al*. 2017). We calculated the normalised Robinson–Foulds (RF) distance between the element and captain phylogenies using the RF.dist function from the phangorn v2.7.0 package (Schliep *et al*. 2017).

We then used a larger dataset of *Starships* predicted using the tool starfish v1.0.0 by Gluck-Thaler and Vogan (2024) to assess whether patterns in the curated kmer tree would persist with broader sampling. Comparisons were made using the entire dataset including elements without predicted flanking repeats (597 elements + 20 *Gaeumannomyces* elements = 617 total) against a filtered dataset of only elements with predicted flanking repeats (343 elements + 14 *Gaeumannomyces* elements = 357 total) to explore the impact of uncertain element boundaries on the topology. For both cases, entire element sequences were again run with Mashtree, but with 100 bootstrap replicates and the default –min-depth parameter to accommodate for the much larger dataset. Previously determined *Starship* family classifications, based on captain phylogenetic relationships (Gluck-Thaler and Vogan 2024), were mapped to element kmer tree tips to visualise the distribution of families across clades using the additional R packages ggtreeExtra v1.10.0 (Xu *et al*. 2021) and glottoTrees v0.1.10 (Round 2021).

Mashtree estimates similarity between kmer sketches using the Mash distance, which models mutation rates under a simple Poisson process of random site mutation (Ondov *et al*. 2016). To compare this with an alternative evolutionary model we used sourmash v4.8.14 (Irber *et al*. 2024) to calculate a distance matrix with the --estimate-ani parameter. Like the Mash distance, average nucleotide identity (ANI) as implemented in sourmash is computed from the Jaccard index, but unlike Mash it does not make the assumption that all kmers are mutated independently, which can result in Mash overestimating mutation rates (Rahman Hera *et al*. 2023). The kmer sketching algorithm within sourmash, FracMinHash, may also outperform Mash's MinHash algorithm when used on very different set sizes (Rahman Hera *et al*. 2023). We should caveat that ANI was developed for use with prokaryote data and has not, to our knowledge, been validated with

eukaryote data, although this may predominantly be due to scalability issues when working with larger eukaryote genomes. We used the ape nj command in R to generate a neighbour-joining tree from the sourmash ANI distance matrix, which is conceptually the same tree-building approach that is integrated into Mashtree.

Exploration of cargo gene content in *Gaeumannomyces* elements

We used the aforementioned larger dataset of twenty *Starships* predicted from seven *Gaeumannomyces* genomes to assess whether similarities in cargo gene content corresponded with the patterns of relatedness described by the kmer trees. We characterised orthologous genes predicted in our previous study (Hill *et al*. 2025) as being core, accessory or specific within the set of twenty elements, and their sharedness was visualised using the R package ComplexUpset v1.3.3 (Krassowski 2022). After normalising cargo orthogroup presence-absence values with the base R scale function, we produced a Euclidean distance matrix using the R dist function and performed hierarchical clustering with the hclust function using the 'complete' agglomeration method. We then compared the topology produced by hierarchical clustering with phylogenetic relationships from the larger kmer-based tree using a tanglegram and calculated the normalised RF distance, as described above. We also determined the location of cargo orthogroups – i.e. whether orthologous genes were only found inside elements or also found in the wider genome.

We searched for specific genes or domains previously reported to be prevalent in *Starships* or with assigned functional roles of particular note (Gluck-Thaler *et al*. 2022) using BLAST v2.10 (Camacho *et al*. 2009) and also PFAM domain assignment from the functional annotation (Hill *et al*. 2025). Namely: DUF3723, ferric reductase (FRE), patatin-like phosphatase (PLP), ToxA effector, spore killing (Spok) genes, and associated domains. We additionally made BLAST searches against the Pathogen–Host Interactions Database v4.17 (PHI-base; (Urban *et al*. 2025) downloaded on 1st August 2024, and considered a positive match when at least 50% of genes in an orthogroup had the same hit. We assessed whether gene ontology (GO) terms were enriched amongst cargo genes using the R package topGO v2.52.0 (Alexa and Rahnenfuhrer 2022) with Fisher's exact test and the weight01 algorithm.

In addition to previously mentioned packages, data analysis and visualisation was performed using the following R packages: cowplot v1.1.3 (Wilke 2024), ggforce v0.4.2 (Pedersen 2024), gggenomes v1.0.0 (Hackl *et al*. 2024), ggnewscale v0.4.10 (Campitelli 2024), ggpubr v0.6.0 (Kassambara 2023),

ggrepel v0.9.5 (Slowikowski 2024), matrixStats v1.3.0 (Bengtsson 2024), patchwork v1.2.0 (Pederson 2024), scales v1.3.0 (Wickham and Seidel 2023), tgutil v0.1.15 (Chomsky and Lifshitz 2023) and tidyverse v2.0.0 (Wickham *et al*. 2019).

RESULTS AND DISCUSSION

A kmer-based approach for *Starship* phylogenetics recovers signal corresponding to host taxonomy

We used a kmer-based approach for phylogenetic analysis of *Starships* to produce a phylogenetic tree of 53 entire *Starship* element sequences from Gluck-Thaler et al. (2022) and Hill et al. (2025), encompassing 17 host genera across 6 classes in the *Pezizomycotina*. We found elements to broadly cluster by genus, even when differing greatly in length (Fig. 1a). This contrasted with the captain gene tree (Supplementary Fig. 1) and element and captain trees were frequently discordant (RF distance 0.73=73% differing bipartitions; Fig. 1b), i.e. *Starships* that were more closely related according to their kmer profiles could have very divergent captain genes. There were some exceptions to element/captain discordance, for instance similar relationships in both captain and element trees were observed for the *Alternaria* clade (Fig. 1b). *Alternaria* captains were also closely related to some *Macrophomina* captains, in reflection of expected host species relationships in the *Dothideomycetes*, however dothideomycete captains were not monophyletic as *Macrophomina* captains were also dispersed across other clades in the captain tree (Supplementary Fig. 1). Overall, 6/10 host genera with more than one genome represented were monophyletic in the element tree versus 2/10 in the captain tree. Also note the placement of Mpha_Derelict – a previously 'unclassifiable' deactivated *Starship* missing the captain gene – alongside other elements from *Macrophomina* species (Fig. 1a). Two striking disruptions of this host clustering were caused by the elements Bdot_Voyager and Pvar_Chrysaor, the latter of which has been recently asserted to be horizontally transferred between various eurotiomycete species (Urquhart *et al*. 2024).

To determine if these observations of clustering by host taxonomy extended more broadly across the *Pezizomycotina*, we used the same kmer-based phylogenetics method on a larger dataset of 597 elements systematically predicted using the tool starfish by Gluck-Thaler et al. (2024) alongside 20 *Gaeumannomyces* elements (Hill *et al*. 2025). This again recovered widescale

clustering by host taxonomy, with the additional clear formation of clades broadly corresponding to host class-level (Fig. 1c; Supplementary Fig. 2). We also performed a more conservative analysis to minimise the risk of including kmers from the background genome, where we filtered the larger dataset to include only elements with predicted flanking direct repeats (343 elements + 14 *Gaeumannomyces* elements), which broadly reflected the results from the unfiltered dataset (Supplementary Fig. 3). As may be expected from the observed element/captain tree discordance in Fig. 1b, family classifications based on captains were scattered across the larger starfish-predicted element kmer trees (Fig. 1d, Supplementary Fig. 2,3). The degree of element/captain phylogenetic discordance is important because phylogenetic relationships of captains have been the predominant factor in element classification (Gluck-Thaler and Vogan 2024).

Phylogenetic discordance in comparison to species relationships is frequently used as evidence for horizontal gene transfer (HGT) (Ravenhall *et al*. 2015), however there are a number of alternative biological and/or analytical factors that can also result in a similar pattern (Steenwyk *et al*. 2023). Trans-species polymorphisms, where polymorphism originates before speciation and is preserved, potentially by balancing selection, can result in genes being more similar between species than within. Trans-species polymorphisms have been reported in fungal genes associated with vegetative incompatibility (Milgroom *et al*. 2018; Auxier *et al*. 2024), and such genes have been found multiple times in *Starships* (Fig. 2a; Gluck-Thaler *et al*. 2022, 2024; Urquhart *et al*. 2024). Even without natural selection, neutral processes such as incomplete lineage sorting; recombination and gene conversion; and gene duplication and loss can elevate levels of discordance (Bjornson *et al*. 2024). The latter is a particularly aggravating factor for misidentifying HGT as it can result in paralogues being mistaken as orthologues (Smith and Hahn 2021).

Another suite of commonly used methods to detect HGT are 'surrogate' phylogenetics methods, which do not build a tree but still assess evolutionary distances e.g. using sequence similarity (Ravenhall *et al*. 2015), however the results of surrogate methods can still be confounded by the phenomena described above. A sequence similarity approach also comes with the caveat that the best BLAST hit is not necessarily the closest related gene (Koski and Golding 2001), and requires subjective decisions about acceptable similarity thresholds. Distinguishing the cause(s) of phylogenetic discordance can be especially difficult for closely related taxa (Steenwyk *et al*. 2023), which is relevant here as elements from different host species were scattered amongst each other within genus-level clades in all kmer-based tree analyses (Fig. 1a, Supplementary Fig. 2). Due to

semipermeable species boundaries in fungi, interspecific hybridisation within the genus level has been detected multiple times (Steenkamp *et al*. 2018; Steensels *et al*. 2021). In such cases, *Starships* could be inherited during sexual reproduction between two different species and subsequent backcrossing could leave the element as an introgression which may be mistaken as having been horizontally transferred. For all the reasons outlined above, general frequency of HGT events may have been overestimated in fungi (Kurland *et al*. 2003; Dupont and Cox 2017). The kmer-based phylogenetics approach described here may be useful in certain contexts as one piece of evidence towards identifying (or dismissing) HGT, but the confounding factors described above would need to be assessed to have confidence that HGT has occurred (e.g. Fijarczyk and Babik 2015; Knowles *et al*. 2018). A number of the above factors contributing to discordant relationships are likely to have a greater impact for more closely related species, and it may be important to focus attention on apparent HGT events across greater evolutionary distances, which are presumed to be rarer, at least in prokaryotes (Popa *et al*. 2017; Burch *et al*. 2023; Dmitrijeva *et al*. 2024).

In the larger kmer-based tree there were many within-genus subclades of elements with captains of the same family, but also cases where minimally diverged sister elements had different captains. For example: aspcri2_s00912 and aspcri1_s00891 from different host genomes within the *Aspergillus*-9 clade had Phoenix and Prometheus captains, respectively; and aspnig6_s01954 and aspnig6_s01955 from the same host genome within the clade Aspergillus-19 had Hephaestus and Phoenix captains, respectively (Supplementary Fig. 2). It should be noted that there is some uncertainty as to the boundaries of these elements, as in these cases elements did not have predicted flanking repeats. A similar observation was made by Gluck-Thaler and Vogan (2024) for *Starship* pairs with near identical cargo 'haplotypes' but different captain-derived families. Together with the fact that captain genes are phylogenetically indistinguishable from 'lone' tyrosine recombinase genes harbouring the DUF3435 domain (Gluck-Thaler *et al*. 2022; Hill *et al*. 2025), this prompts the question as to whether *Starships* can swap the captain for a different tyrosine recombinase gene, which would render the 'captain' status as somewhat transient. A previous study has already reported that *Starship* elements can lose their captain gene to become 'degraded' or 'derelict' (Gluck-Thaler *et al*. 2022), and in another study a mechanism has been suggested wherein different elements partake in cargo swapping (Urquhart *et al*. 2024). A similar mechanism where the captain, as opposed to the cargo, is swapped to acquire a captain gene from a different family could be a strategy to diversify insertions of virtually identical elements into different target sites. Comparing the kmer profiles of regions surrounding CMEs could incidentally

be another fruitful avenue for understanding target site preference, as many *Starships* have been found to insert into other TEs and AT-rich regions but without clear patterns in, for instance, TE superfamily or domain (Gluck-Thaler and Vogan 2024).

Aside from the major clade in the larger starfish kmer tree overrepresented with elements from eurotiomycete hosts, other eurotiomycete elements appeared scattered amongst other clades, although there were lower support values for deeper tree nodes (Fig. 1c). It is notable that eurotiomycete elements dominate the starfish dataset – of all the genomes explored by Gluck-Thaler and Vogan (2024), *Eurotiomycetes* was the class with the highest proportion of genomes returning a *Starship* (36%; Supplementary Fig. 4). This was closely followed by the *Orbiliomycetes* (28%), despite 16 times fewer orbiliomycete genomes having been surveyed compared to the *Eurotiomycetes*, and orbiliomycete element clades were similarly widespread across the kmer tree (Fig. 1c). As one of the earliest diverging classes within the *Pezizomycotina* subphylum, the *Orbiliomycetes* are distantly related to *Eurotiomycetes* (Li *et al*. 2021), and they do not share ecological distributions more so than other taxonomic classes, so the underlying biological explanation is unclear. The far larger *Eurotiomycetes* class comprises diverse lifestyles including rock-inhabiting fungi and other extremophiles; plant and animal pathogens; lichenised and lichen-associated fungi; ectomycorrhizal fungi; ant mutualists; and saprotrophs (Geiser *et al*. 2015). The *Orbiliomycetes* are primarily thought to be saprotrophs but include some soil-dwelling carnivorous fungi which trap invertebrates (Pfister 2015). Variation in the rate of *Starship* recovery in the genomes of different taxonomic classes could be a result of inconsistencies in assembly quality, or bias within the starfish tool to recover certain elements from certain classes. However, these results do suggest that there may be a relationship between the tendency for a taxonomic class to have *Starship* elements and greater diversity of element clades.

While we consider this to be a promising application for kmer-based phylogenetics, we must note that such methods were typically developed for whole-genome data. We are not aware of kmer-based phylogenetic methods having been tested on sequences such as fungal CMEs. However, given that such methods are considered well-suited to viral genomes due to their high levels of mutation, gene duplication and rearrangement (Zielezinski *et al*. 2017), CMEs would appear to be a similarly appropriate use-case. Other than circumventing issues with alignment, kmer-based methods also have the advantage of being more computationally efficient than alignment-based phylogenetic methods, which could reduce the carbon footprint of analyses (Grealey *et al*. 2022).

There are many different approaches and tools for alignment-free sequence comparison which would warrant further testing in the context of CME phylogenetics (Luczak *et al*. 2019; Zielezinski *et al*. 2019). For instance, average nucleotide identity (ANI) is frequently used as a distance metric for prokaryote genomes and, as implemented in sourmash, has the benefit of a more realistic evolutionary model of mutation than that used by Mash (Rahman Hera *et al*. 2023), but whether it is appropriate for eukaryote data has yet to be validated. Nonetheless, we found that trees generated from ANI distance matrices produced using sourmash were broadly consistent with our Mashtree results (Supplementary Fig. 5,6) and supported our conclusion that *Starships* predominantly cluster according to host taxonomy. We were unable to produce a kmer tree for captain genes using Mashtree, presumably due to the much smaller sequence length of a single gene. This meant we were not able to directly compare whole element and captain trees using the same kmer-based method. However, at the genome-scale, previous comparisons of alignment and kmer methods suggest reasonable topological congruence (VanWallendael and Alvarez 2022; Lo *et al*. 2022; Van Etten *et al*. 2023), or no greater incongruence than might be expected from using different alignment-based methods (e.g. Shen *et al*. 2021). This also demonstrates the capacity for kmer-based methods to reconstruct evolutionary history and, when they incorporate models of evolution, be deemed 'phylogenetic'.

There are some limitations to alignment-free phylogenetics methods. Unlike conventional alignment-based phylogenetic trees, alignment-free trees do not produce branch lengths with a scale corresponding to geological time, and so one cannot extrapolate the date of divergences. Alignment-free methods also struggle with the reconstruction of deep nodes (Fan *et al*. 2015), which is evident from the kmer trees we present here, although that issue is inherent to all phylogenetics methods (Lanier and Knowles 2015). This may limit the ability of these methods to address questions about inter-relatedness of larger CME clades but should still allow for assessment of more recent divergences.

Both cargo genes and non-coding cargo content contribute to kmer-based phylogenetic relationships between *Gaeumannomyces Starships*

To explore the extent to which cargo gene content corresponded with the kmer-based phylogenetic relationships, we used twenty *Starships* previously identified from seven genomes across three separate lineages within the genus *Gaeumannomyces,* an understudied member of the *Magnaporthaceae* (Hill *et al*. 2025). These genomes were sequenced from five strains of the wheat

root pathogen species *G. tritici* (*Gt*) and two of the oat root pathogen *G. avenae* (*Ga*). Within the *Gt* strains there is further subdivision of two strains belonging to 'type A' and three to 'type B', two distinct genetic lineages present in the species (Palma-Guerrero *et al*. 2021). This division is meaningful, as differences between the two types in terms of both virulence and genomic signatures may indicate that these two types actually represent cryptic species (Hill *et al*. 2025). As well as being a consistently amassed set of *Starships* for controlled comparison, these *Gaeumannomyces* elements also provided major variability, ranging from ~32–688 Kbp in total length and containing between 1–156 genes (Fig. 2a). It should be noted that six of the elements, including both from the *Gt*A strains, were excluded from the first phylogenetic analysis (Fig. 1a) as these elements did not have predicted flanking direct repeats and so there is some uncertainty as to their exact boundaries. However, we retain them here so as not to exclude potentially biologically meaningful results.

We found that *Starships* with greater numbers of shared orthologous genes were frequently sister elements or closely related in the kmer tree, for instance Gt-LH10_s00088, Gt-23d_s00104 and Ga-3aA1_s00046 (Fig. 3a). Most cases of more distantly related elements with high cargo gene sharedness involved the largest and most gene-rich element, Gt-23d_s00107, which incidentally also had one of the highest proportions (48%) of element-specific genes. Hierarchical clustering of cargo orthologous gene content supported these results, with reasonable concordance between the hierarchical clustering and kmer element tree (RF distance 0.47=47% differing bipartitions; Fig. 3c) and the most notable deviation between the two trees was the divergence of element Gt-23d_s00107. Pairs of closely related elements with evident regions of syntenic cargo genes (Fig. 2a) were often located on different chromosomes, suggesting previous mobilisation (e.g. Gt-23d_s00104 and Ga-3aA1_s00046; Ga-CB1_s00036 and Ga-3aA1_s00044; Gt-4e_s00056 and Gt-23d_s00105; Fig. 2b). In contrast, there were also apparently static elements, being closely related and in the same orientation and position within different genomes (e.g. Gt-LH10_s00088 and Ga-3aA1_s00046; Gt-4e_s00058 and Gt-23d_s00103). The question of how similar elements must be to be considered 'the same' is also pertinent, as there was one case of closely related elements at different locations within the same host genome, although one lacking predicted flanking repeats (Gt-23d_s00105 and Gt-23d_s00099). Elements becoming multi-copy in the genome may arise from mobilisation of an ancestral element followed by sexual recombination between two hosts with the element in the original and more recent genomic location, respectively (Urquhart *et al*. 2023).

While cargo gene content was evidently a contributing factor to the patterns of *Gaeumannomyces* element relatedness recovered from the kmer-based phylogenies, the nature of a kmer-based approach means that intergenic content within *Starships* must also be implicated. Indeed, repetitive DNA, introns and presumably other non-coding regions can provide important phylogenetic signals (Lo *et al*. 2022). Here, the only two *Gt*A elements found, one in each *Gt*A genome, contained a single cargo gene despite being 61 and 73 Kbp long. In the larger kmer tree of starfish-predicted elements the *Gt*B and *Ga* elements were closely related to sordariomycete elements from the pathogenic rice blast fungus *Pyricularia oryzae* (syn. *Magnaporthe oryzae*) and a eurotiomycete clade, while the single-gene *Gt*A elements were in a distinct clade more closely related to an element from the sordariomycete species *Sporothrix brasiliensis*, albeit without significant branch support (Supplementary Fig. 2). *S. brasiliensis* is found in soils and vegetation, but is also an opportunistic mammalian pathogen, primarily of humans and cats, due to its temperature-dependent dimorphic lifestyle (Téllez *et al*. 2014). Despite being a similar length (57 Kbp) to the *Gt*A elements, the *S. brasiliensis* element contained 19 genes, none of which showed sequence similarity with the single gene found in the *Gt*A elements. This suggests that it was primarily non-coding cargo content that informed kmer-based relationships between the *S. brasiliensis* and *Gt*A elements. The *Gt*A elements were also previously found to have likely undergone repeat-induced point mutation (RIP) (Hill *et al*. 2025). RIP induces transition mutations in repetitive DNA, with a particular bias for C→T mutations targeting CpA dinucleotides, and so RIP-like signatures in genomic sequences manifest as biases in the relative frequencies of dinucleotides (Lewis *et al*. 2009; Hane *et al*. 2015). This raises the question of whether or to what extent signatures of RIP, such as a higher frequency of TpA dinucleotides, influence kmer-based inference of element relationships, especially in cases with extensive intergenic cargo content.

The whole-element kmer trees, captain tree and the patterns of shared cargo genes indicated that there is no apparent species boundary for *Starship* content between *Gt*B and *Ga*. We found no evidence of similarity with *Gt*A elements, although there was only one gene-poor *Gt*A element with which to compare. We see two possible scenarios: (1) elements were in the common ancestor of all three lineages and lost in *Gt*A or (2) elements are readily exchanged between *Ga* and *Gt*B strains, whether through HGT or interspecific hybridisation. Either way, together with the fact that, unlike the other *Gaeumannomyces* elements, the *Gt*A elements were previously found to be subject to element-wide RIP (Hill *et al*. 2025), *Starship* prevalence and divergence may be another symptom of cryptic speciation between *Gt* types. Although *Gt*B and *Ga* elements appear to be closely related,

there was an imbalance in how cargo genes were shared, as a higher proportion of *Ga* cargo genes had an orthologue in *Gt*B elements (56%) than *Gt*B cargo genes had in *Ga* elements (38%; Fig. 3b). Additionally, there were differences in how cargo genes were distributed in the genome, with more cargo gene orthogroups only found inside *Ga* elements that had copies integrated into the wider genome in *Gt* strains than the reverse (Supplementary Fig. 8a). In a similar vein, *Ga Starships* broadly had a higher proportion of orthogroups that were only inside the element compared to *Gt*B *Starships* (Supplementary Fig. 8b). Unpicking the differences in relative levels of duplication, sharedness and location of cargo genes on different *Starships* may be important for determining patterns of inheritance or selection.

Gaeumannomyces Starship cargos harbour a variety of putative plant–fungal interaction genes, but the ToxA gene was notably absent

Most genes previously reported to be common, or notable, in *Starships* (Gluck-Thaler *et al*. 2022) were absent from *Gaeumannomyces Starship* cargos, namely DUF3723, ferric reductase (FRE), patatin-like phosphatase (PLP) and spore-killer (Spok1) genes. There was one putative NOD-like receptor (NLR) located on element Gt-23d_s00107 (Fig. 2). The NLR contained a central NACHT domain – the most common nucleotide binding and oligomerization (NOD) domain in fungal NLRs (Daskalov *et al*. 2020) – a WD40 repeat domain, and a sesA N-terminal domain of unknown function (PF17107) that is more common in ascomycete NLRs (Daskalov *et al*. 2020). This sesA-NACHT-WD structure is also found in the NWD3 gene of the model experimental fungus *Podospora anserina* (Daskalov *et al*. 2012). While the function of sesA is not established, other members of the *P. anserina* NWD gene family are involved in heterokaryon/vegetative incompatibility or self/non-self recognition, which has also been hypothesised to contribute to an innate fungal immune system (Paoletti and Saupe 2009; Uehling *et al*. 2017).

Of particular note was the absence of the necrosis-inducing ToxA effector in the *Gaeumannomyces* cargos, which is located in *Starships* in three other wheat pathogens – *Pyrenophora tritici-repentis, Parastagonospora nodorum* and *Bipolaris sorokiniana* (McDonald *et al*. 2019; Bucknell *et al*. 2024). *Py. tritici-repentis* and *Pa. nodorum* are known to frequently co-infect wheat (Abdullah *et al*. 2020), and *Py. tritici-repentis* and *B. sorokiniana* together form a leaf blight disease complex (Kumar *et al*. 2002). While we could not find information on potential co-occurrence of *Gaeumannomyces* spp. and other wheat pathogens in the literature, based on their global distributions and the global distribution of the wheat crop, it is highly likely that *Gaeumannomyces* spp. also cooccur with one

or more of these wheat pathogens (Větrovský *et al*. 2020), which would have provided the opportunity to exchange *Starships*. However, all three species containing ToxA reside in a different class, *Dothideomycetes*, in the order *Pleosporales*. At the present time, the lack of ToxA in the *Gaeumanomyces Starships* is consistent with our kmer tree results indicating a host relatedness boundary to *Starship* exchange.

Regarding whether the *Gaeumannomyces Starship* cargos exhibited a core functional role, GO term enrichment analysis of cargo genes reflected high variability as there was no significant enrichment in most elements, although ubiquinone biosynthesis and regulation of translational fidelity were significantly enriched in Ga-3aA1_s00044 and Ga-CB1_s00036, respectively. There were no cargo orthogroups that were core to all elements, but five orthogroups were present in at least 50% of the elements (Supplementary Fig. 7). One was predicted to be a carbohydrate-active enzyme (CAZyme) belonging to glycosyltransferase family 2 (GT2; Fig. 2). The GT2 family includes enzymes necessary for the synthesis of chitin (Lairson *et al*. 2008), which is required for structural integrity of the fungal cell wall (Bowman and Free 2006). A GT2 enzyme has been demonstrated to be required for the disease-causing abilities of the wheat pathogens *Zymoseptoria tritici* and *Fusarium graminearum* (King *et al*. 2017). Expansion and contraction of GT2 CAZyme genes have been shown to be strong predictors of phytopathogenicity and saprotrophy, respectively (Dort *et al*. 2023), but GT2 genes are also expanded in mycorrhizal lineages (Rosling *et al*. 2024), suggesting a key role in both pathogenic and mutualistic plant–fungal interactions. In addition to the prevalent GT2 orthogroup, other CAZymes and CAZyme families were found in various elements: sterol 3 β-glucosyltransferase (GT1), glycoside hydrolase (GH) family 33, α-galactosidase (CBM35+GH27), and glucose-methanol-choline oxidoreductase (AA3_2) in elements Ga-3aA1_s00044 and Ga-CB1_s00036; chitinase (GH18) in Gt-LH10_s00085; and another GT2 CAZyme in Gt-23d_s00099.

Multiple *Gaeumannomyces Starship* cargo genes had BLAST hits to genes in the PHI-base database, which compiles and curates experimentally verified genes implicated in pathogen–host interactions (Urban *et al*. 2025). This included four genes in the closely related *P. oryzae* which have been associated with virulence in barley and rice, two of which are implicated in calcium signalling and two transcription factors, and the previously mentioned GT2 CAZyme which has been associated with virulence of *Zymoseptoria tritici* and *Fusarium graminearum* in wheat leaves and floral spikes, respectively (Table 1). Intriguingly, the chitinase CAZyme cargo gene in element Gt-LH10_s00085 matched a chitinase gene in the mycoparasite *Trichoderma virens* which is

associated with its virulence towards the basidiomycete plant pathogen *Rhizoctonia solani*. *Trichoderma* species are known for endophytic colonisation of plants, particularly roots, and in some cases can reduce disease via both inducing plant resistance and direct antagonism of other fungi (Harman *et al*. 2004). Two further orthogroups had BLAST hits to CAZyme genes in PHI-base (Xyp1 and PELB/CcpelA), however as these were not previously flagged during CAZyme annotation (Hill *et al*. 2025) there remains some uncertainty as to their function.

Also of note is that none of the biosynthetic gene clusters (BGCs) previously identified in the *Gaeumannomyces* genomes were present in any *Starships*, but two cargo genes had hits to PHI-base genes implicated in secondary metabolite synthesis in *Fusarium* species, namely nrps5 and FUG1. The latter is involved in fumonisin synthesis in *Fusarium verticillioides* (Ridenour and Bluhm 2017), but is located on a separate locus to the fumonisin (FUM) gene cluster, suggesting that it may play a regulatory role, as biosynthesis transcription factors can frequently be located outside of contiguous BGCs (Kwon *et al*. 2021). FUG1 was also previously found to have orthologues across *Ascomycota*, including in *Gt* (Ridenour and Bluhm 2017). The non-ribosomal peptide synthetase nrps5 gene is located alongside nrps9 in an eight-member BGC cluster in *Fusarium* species, which produces fusaoctaxin A and is essential to virulence of *F. graminearum* in wheat (Jia *et al*. 2019). However, none of the genes surrounding the nrps5-like gene in the *Gaeumannomyces* elements showed similarity to the other nrps5/9 cluster members. We also found an uncharacterised candidate secreted effector protein (CSEP) gene in one element (Ga-CB1_s00036). Intriguingly this CSEP was located within a region that was highly syntenic with another element (Ga-3aA1_s00044) but the CSEP was not present in that second element (Fig. 2), underlining the dynamism of *Starship* cargos.

Conclusions

Here, we provide evidence of a difference in evolutionary history between *Starship* elements in their entirety versus their captain genes. This raises the question: is it more important to define *Starships* by their mode of mobilisation – i.e. the tyrosine recombinase captain gene – or the cargo of genes and non-coding/repetitive content mobilised? The answer to that question will depend on the context in which the question is asked; namely, whether the enquiry at hand is to understand the mechanism of transposition, or to understand how elements and their cargos evolve and impact

host fitness. Whole-element relationships are easily assessed using kmer-based phylogenetic methods, which has revealed previously hidden signals corresponding to host taxonomy. These methods also allow us to assess relationships including 'degraded' elements where captain and/or DRs/TIRs have been lost. By accounting for the composition of *Starships* without being hampered by alignment issues caused by repeats, indels, duplications, rearrangements and inversions, or lack of available sequences in general, kmer-based phylogenetic methods can help to refine the existing haplotype-based classification of CMEs. Beyond informing classification, this new approach could also provide context and new insights to address fundamental outstanding questions regarding *Starships* and other CMEs, such as the evolutionary origins of elements, the prevalence of HGT and the role of elements in the host genome.

DATA AVAILABILITY STATEMENT

All original data sources used in this study are cited in the text. Analysis scripts are available at https://github.com/Rowena-h/StarshipTrees.

ACKNOWLEDGMENTS

We are very grateful to Gillian Reynolds at the Earlham Institute for sharing her insights on kmer-based methods. Many thanks to Javier Palma-Guerrero and Tania Chancellor for valuable discussion as part of the bilateral Earlham Institute–Rothamsted Research take-all working group. We also thank Neil Hall at the Earlham Institute for his continued support and guidance.

FUNDING

RH, GC, MG, KHK and MM were supported by the Biotechnology and Biological Sciences Research Council (BBSRC) Institute Strategic Programme (ISP) grant, Delivering Sustainable Wheat (BB/X011003/1) within the work package Delivering Resilience to Biotic Stress (BBS/E/ER/230003B Earlham Institute and BBS/E/RH/230001B Rothamsted Research). DS was supported by the BBSRC ISP Grant (BB/CCG2280/1). GC was supported by the DEFRA funded Wheat Genetic Improvement Network (WGIN) phase 3 (CH0106) and phase 4 (CH0109). MG was supported by the BBSRC ISP grant Decoding Biodiversity (BBX011089/1) within the work package Genome Enabled Analysis of Diversity to Identify Gene Function, Biosynthetic Pathways, and Variation in Agricultural Traits (BBS/E/ER/230002B).

REFERENCES

Abdullah AS, Gibberd MR and Hamblin J. 2020. Co-infection of wheat by *Pyrenophora tritici-repentis* and *Parastagonospora nodorum* in the wheatbelt of Western Australia. Crop Pasture Sci 71: 119–127. doi:10.1071/CP19412.

Alexa A and Rahnenfuhrer J. 2022. topGO: Enrichment Analysis for Gene Ontology. https://bioconductor.org/packages/release/bioc/html/topGO.html.

Arkhipova IR and Yushenova IA. 2019. Giant Transposons in Eukaryotes: Is Bigger Better? Genome Biol Evol 11: 906–918. doi:10.1093/gbe/evz041.

Auxier B, Zhang J, Marquez FR, Senden K, Van Den Heuvel J, Aanen DK, Snelders E and Debets AJM. 2024. The Narrow Footprint of Ancient Balancing Selection Revealed by Heterokaryon Incompatibility Genes in *Aspergillus fumigatus*. Molecular Biology and Evolution 41: msae079. doi:10.1093/molbev/msae079.

Bengtsson H. 2024. matrixStats: Functions that Apply to Rows and Columns of Matrices (and to Vectors). https://cran.r-project.org/package=matrixStats.

Biémont C. 2010. A Brief History of the Status of Transposable Elements: From Junk DNA to Major Players in Evolution. Genetics 186: 1085–1093. doi:10.1534/genetics.110.124180.

Bjornson S, Verbruggen H, Upham NS and Steenwyk JL. 2024. Reticulate evolution: Detection and utility in the phylogenomics era. Molecular Phylogenetics and Evolution 201: 108197. doi:10.1016/j.ympev.2024.108197.

Bowman SM and Free SJ. 2006. The structure and synthesis of the fungal cell wall. BioEssays 28: 799–808. doi:10.1002/bies.20441.

Bucknell A, Wilson HM, Gonçalves Do Santos KC, Simpfendorfer S, Milgate A, Germain H, Solomon PS, Bentham A and McDonald MC. 2024. *Sanctuary*: A *Starship* transposon facilitating the movement of the virulence factor ToxA in fungal wheat pathogens. bioRxiv. doi:10.1101/2024.03.04.583430.

Burch CL, Romanchuk A, Kelly M, Wu Y and Jones CD. 2023. Empirical Evidence That Complexity Limits Horizontal Gene Transfer. Genome Biol Evol 15: evad089. doi:10.1093/gbe/evad089.

Camacho C, Coulouris G, Avagyan V, Ma N, Papadopoulos J, Bealer K and Madden TL. 2009. BLAST+: architecture and applications. BMC Bioinformatics 10: 421. doi:10.1186/1471-2105-10-421.

Campitelli E. 2024. ggnewscale: Multiple Fill and Colour Scales in "ggplot2." https://cran.r-project.org/package=ggnewscale.

Capella-Gutiérrez S, Silla-Martínez JM and Gabaldón T. 2009. trimAl: a tool for automated alignment trimming in large-scale phylogenetic analyses. Bioinformatics 25: 1972–1973. doi:10.1093/bioinformatics/btp348.

Chancellor T, Smith DP, Chen W, Clark SJ, Venter E, Halsey K, Carrera E, McMillan V, Canning G, Armer VJ, *et al.* 2024. A fungal endophyte induces local cell wall–mediated resistance in wheat roots against take-all disease. Front Plant Sci 15: 1444271. doi:10.3389/fpls.2024.1444271.

Chomsky E and Lifshitz A. 2023. tgutil: Simple utility functions for Tanay lab code. https://github.com/tanaylab/tgutil.

Daskalov A, Dyrka W and Saupe SJ. 2020. 6 NLR Function in Fungi as Revealed by the Study of Self/Non-self Recognition Systems, pp. 123–141 in *Genetics and Biotechnology*, edited by J. P. Benz and K. Schipper. The Mycota, Springer International Publishing, Cham. doi:10.1007/978-3-030-49924-2_6.

Daskalov A, Paoletti M, Ness F and Saupe SJ. 2012. Genomic Clustering and Homology between HET-S and the NWD2 STAND Protein in Various Fungal Genomes. PLoS ONE 7: e34854. doi:10.1371/journal.pone.0034854.

Dmitrijeva M, Tackmann J, Matias Rodrigues JF, Huerta-Cepas J, Coelho LP and von Mering C. 2024. A global survey of prokaryotic genomes reveals the eco-evolutionary pressures driving horizontal gene transfer. Nat Ecol Evol 8: 986–998. doi:10.1038/s41559-024-02357-0.

Dort EN, Layne E, Feau N, Butyaev A, Henrissat B, Martin FM, Haridas S, Salamov A, Grigoriev IV, Blanchette M, *et al.* 2023. Large-scale genomic analyses with machine learning uncover predictive patterns associated with fungal phytopathogenic lifestyles and traits. Sci Rep 13: 17203. doi:10.1038/s41598-023-44005-w.

Dupont P-Y and Cox MP. 2017. Genomic Data Quality Impacts Automated Detection of Lateral Gene Transfer in Fungi. G3: Genes, Genomes, Genetics 7: 1301–1314. doi:10.1534/g3.116.038448.

Fan H, Ives AR, Surget-Groba Y and Cannon CH. 2015. An assembly and alignment-free method of phylogeny reconstruction from next-generation sequencing data. BMC Genomics 16: 522. doi:10.1186/s12864-015-1647-5.

Fijarczyk A and Babik W. 2015. Detecting balancing selection in genomes: limits and prospects. Molecular Ecology 24: 3529–3545. doi:10.1111/mec.13226.

Geiser DM, LoBuglio KF and Gueidan C. 2015. 5 Pezizomycotina: Eurotiomycetes, pp. 121–141 in *Systematics and Evolution*, edited by D. J. McLaughlin and J. W. Spatafora. The Mycota 7B, Springer Berlin Heidelberg, Berlin, Heidelberg. doi:10.1007/978-3-662-46011-5_5.

Gluck-Thaler E, Forsythe A, Puerner C, Stajich JE, Croll D, Cramer RA and Vogan AA. 2024. Giant transposons promote strain heterogeneity in a major fungal pathogen. doi:10.1101/2024.06.28.601215.

Gluck-Thaler E, Ralston T, Konkel Z, Ocampos CG, Ganeshan VD, Dorrance AE, Niblack TL, Wood CW, Slot JC, Lopez-Nicora HD, *et al.* 2022. Giant *Starship* Elements Mobilize Accessory Genes in Fungal Genomes. Mol Biol Evol 39: msac109. doi:10.1093/molbev/msac109.

Gluck-Thaler E and Vogan AA. 2024. Systematic identification of cargo -mobilizing genetic elements reveals new dimensions of eukaryotic diversity. Nucleic Acids Res 1–18. doi:10.1093/nar/gkae327.

Goodwin TJD, Butler MI and Poulter RTM. 2003. Cryptons: a group of tyrosine-recombinase-encoding DNA transposons from pathogenic fungi. Microbiology 149: 3099–3109. doi:10.1099/mic.0.26529-0.

Grealey J, Lannelongue L, Saw W-Y, Marten J, Méric G, Ruiz-Carmona S and Inouye M. 2022. The Carbon Footprint of Bioinformatics. Mol Biol Evol 39: msac034. doi:10.1093/molbev/msac034.

Hackl T, Ankenbrand MJ and van Adrichem B. 2024. gggenomes: A Grammar of Graphics for Comparative Genomics. https://github.com/thackl/gggenomes.

Hane JK, Williams AH, Taranto AP, Solomon PS and Oliver RP. 2015. Repeat-Induced Point Mutation: A Fungal-Specific, Endogenous Mutagenesis Process, pp. 55–68 in *Genetic Transformation Systems in Fungi*, edited by M. A. van den Berg and K. Maruthachalam. Fungal Biology, Springer International Publishing. doi:10.1007/978-3-319-10503-1_4.

Harman GE, Howell CR, Viterbo A, Chet I and Lorito M. 2004. *Trichoderma* species — opportunistic, avirulent plant symbionts. Nat Rev Microbiol 2: 43–56. doi:10.1038/nrmicro797.

Hill R, Grey M, Fedi MO, Smith D, Canning G, Ward SJ, Irish N, Smith J, McMillan VE, Hammond J, *et al.* 2025. Evolutionary genomics reveals variation in structure and genetic content implicated in virulence and lifestyle in the genus *Gaeumannomyces*. BMC Genomics 26: 239. doi:10.1186/s12864-025-11432-0.

Irber L, Pierce-Ward NT, Abuelanin M, Alexander H, Anant A, Barve K, Baumler C, Botvinnik O, Brooks P, Dsouza D, *et al.* 2024. sourmash v4: A multitool to quickly search, compare,and analyze genomic and metagenomic data sets. JOSS 9: 6830. doi:10.21105/joss.06830.

Jia L-J, Tang H-Y, Wang W-Q, Yuan T-L, Wei W-Q, Pang B, Gong X-M, Wang S-F, Li Y-J, Zhang D, *et al.* 2019. A linear nonribosomal octapeptide from *Fusarium graminearum* facilitates cell-to-cell invasion of wheat. Nat Commun 10: 922.

Kassambara A. 2023. ggpubr: "ggplot2" Based Publication Ready Plots. https://cran.r-project.org/package=ggpubr.

Katoh K and Standley DM. 2013. MAFFT Multiple Sequence Alignment Software Version : Improvements in Performance and Usability. Mol Biol Evol 30: 772–780. doi:10.1093/molbev/mst010.

Katz LS, Griswold T, Morrison SS, Caravas JA, Zhang S, den Bakker HC, Deng X and Carleton HA. 2019. Mashtree: a rapid comparison of whole genome sequence files. JOSS 4: 1762. doi:10.21105/joss.01762.

King R, Urban M, Lauder RP, Hawkins N, Evans M, Plummer A, Halsey K, Lovegrove A, Hammond-Kosack K and Rudd JJ. 2017. A conserved fungal glycosyltransferase facilitates pathogenesis of plants by enabling hyphal growth on solid surfaces. PLoS Pathog 13: e1006672. doi:10.1371/journal.ppat.1006672.

Knowles LL, Huang H, Sukumaran J and Smith SA. 2018. A matter of phylogenetic scale: Distinguishing incomplete lineage sorting from lateral gene transfer as the cause of gene tree discord in recent versus deep diversification histories. American J of Botany 105: 376–384. doi:10.1002/ajb2.1064.

Kojima KK and Jurka J. 2011. *Crypton* transposons: identification of new diverse families and ancient domestication events. Mobile DNA 2: 12. doi:10.1186/1759-8753-2-12.

Koski LB and Golding GB. 2001. The Closest BLAST Hit Is Often Not the Nearest Neighbor. J Mol Evol 52: 540–542. doi:10.1007/s002390010184.

Kozlov AM, Darriba D, Flouri T, Morel B and Stamatakis A. 2019. RAxML-NG: a fast, scalable and user-friendly tool for maximum likelihood phylogenetic inference. Bioinformatics 35: 4453–4455. doi:10.1093/bioinformatics/btz305.

Krassowski M. 2022. ComplexUpset. https://github.com/krassowski/complex-upset/tree/v1.3.5.

Kumar J, Schäfer P, Hückelhoven R, Langen G, Baltruschat H, Stein E, Nagarajan S and Kogel K. 2002. *Bipolaris sorokiniana*, a cereal pathogen of global concern: cytological and molecular approaches towards better control‡. Mol Plant Pathol 3: 185–195. doi:10.1046/j.1364-3703.2002.00120.x.

Kurland CG, Canback B and Berg OG. 2003. Horizontal gene transfer: A critical view. Proc. Natl. Acad. Sci. U.S.A. 100: 9658–9662. doi:10.1073/pnas.1632870100.

Kwon MJ, Steiniger C, Cairns TC, Wisecaver JH, Lind AL, Pohl C, Regner C, Rokas A and Meyer V. 2021. Beyond the Biosynthetic Gene Cluster Paradigm: Genome-Wide Coexpression Networks Connect Clustered and Unclustered Transcription Factors to Secondary Metabolic Pathways. Microbiol Spectr 9: e00898-21. doi:10.1128/Spectrum.00898-21.

Lairson LL, Henrissat B, Davies GJ and Withers SG. 2008. Glycosyltransferases: Structures, Functions, and Mechanisms. Annu Rev Biochem 77: 521–555. doi:10.1146/annurev.biochem.76.061005.092322.

Lanier HC and Knowles LL. 2015. Applying species-tree analyses to deep phylogenetic histories: Challenges and potential suggested from a survey of empirical phylogenetic studies. Molecular Phylogenetics and Evolution 83: 191–199. doi:10.1016/j.ympev.2014.10.022.

Lewis ZA, Honda S, Khlafallah TK, Jeffress JK, Freitag M, Mohn F, Schübeler D and Selker EU. 2009. Relics of repeat-induced point mutation direct heterochromatin formation in *Neurospora crassa*. Genome Res. 19: 427–437. doi:10.1101/gr.086231.108.

Li Y, Steenwyk JL, Chang Y, Wang Y, James TY, Stajich JE, Spatafora JW, Groenewald M, Dunn CW, Hittinger CT, *et al*. 2021. A genome-scale phylogeny of the kingdom Fungi. Curr Biol 31: 1653–1665. doi:10.1016/j.cub.2021.01.074.

Lo R, Dougan KE, Chen Y, Shah S, Bhattacharya D and Chan CX. 2022. Alignment-Free Analysis of Whole-Genome Sequences From Symbiodiniaceae Reveals Different Phylogenetic Signals in Distinct Regions. Front Plant Sci 13: 815714. doi:10.3389/fpls.2022.815714.

Luczak BB, James BT and Girgis HZ. 2019. A survey and evaluations of histogram-based statistics in alignment-free sequence comparison. Brief Bioinform 20: 1222–1237. doi:10.1093/bib/bbx161.

McDonald MC, Taranto AP, Hill E, Schwessinger B, Liu Z, Simpfendorfer S, Milgate A and Solomon PS. 2019. Transposon-Mediated Horizontal Transfer of the Host-Specific Virulence Protein ToxA between Three Fungal Wheat Pathogens. mBio 10: e01515-19. doi:10.1128/mBio.01515-19.

Milgroom MG, Smith ML, Drott MT and Nuss DL. 2018. Balancing selection at nonself recognition loci in the chestnut blight fungus, *Cryphonectria parasitica*, demonstrated by trans-species polymorphisms, positive selection, and even allele frequencies. Heredity 121: 511–523. doi:10.1038/s41437-018-0060-7.

Ondov BD, Treangen TJ, Melsted P, Mallonee AB, Bergman NH, Koren S and Phillippy AM. 2016. Mash: fast genome and metagenome distance estimation using MinHash. Genome Biol 17: 132. doi:10.1186/s13059-016-0997-x.

Palma-Guerrero J, Chancellor T, Spong J, Canning G, Hammond J, McMillan VE and Hammond-Kosack KE. 2021. Take-All Disease: New Insights into an Important Wheat Root Pathogen. Trends Plant Sci 26: 836–848. doi:10.1016/j.tplants.2021.02.009.

Paoletti M and Saupe SJ. 2009. Fungal incompatibility: Evolutionary origin in pathogen defense? BioEssays 31: 1201–1210. doi:10.1002/bies.200900085.

Paradis E and Schliep K. 2019. Ape 5.0: An environment for modern phylogenetics and evolutionary analyses in R. Bioinformatics 35: 526–528. doi:10.1093/bioinformatics/bty633.

Pedersen TL. 2024. ggforce: Accelerating “ggplot2.” https://cran.r-project.org/web/packages/ggforce/index.html.

Pederson TL. 2024. patchwork: The Composer of Plots. https://CRAN.R-project.org/package=patchwork.

Pfister DH. 2015. 2 Pezizomycotina: Pezizomycetes, Orbiliomycetes, pp. 35–55 in *Systematics and Evolution*, edited by D. J. McLaughlin and J. W. Spatafora. The Mycota 7B, Springer Berlin Heidelberg, Berlin, Heidelberg. doi:10.1007/978-3-662-46011-5_2.

Popa O, Landan G and Dagan T. 2017. Phylogenomic networks reveal limited phylogenetic range of lateral gene transfer by transduction. The ISME Journal 11: 543–554. doi:10.1038/ismej.2016.116.

R Core Team. 2023. R: A language and environment for statistical computing. https://www.r-project.org/.

Rahman Hera M, Pierce-Ward NT and Koslicki D. 2023. Deriving confidence intervals for mutation rates across a wide range of evolutionary distances using FracMinHash. Genome Res. 33: 1061–1068. doi:10.1101/gr.277651.123.

Ravenhall M, Škunca N, Lassalle F and Dessimoz C. 2015. Inferring Horizontal Gene Transfer (S. Wodak, Ed.). PLoS Comput Biol 11: e1004095. doi:10.1371/journal.pcbi.1004095.

Revell LJ. 2024. phytools 2.0: an updated R ecosystem for phylogenetic comparative methods (and other things). PeerJ 12: e16505. doi:10.7717/peerj.16505.

Ridenour JB and Bluhm BH. 2017. The novel fungal-specific gene *FUG1* has a role in pathogenicity and fumonisin biosynthesis in *Fusarium verticillioides*. Mol Plant Pathol 18: 513–528. doi:10.1111/mpp.12414.

Rosling A, Eshghi Sahraei S, Kalsoom Khan F, Desirò A, Bryson AE, Mondo SJ, Grigoriev IV, Bonito G and Sánchez-García M. 2024. Evolutionary history of arbuscular mycorrhizal fungi and genomic signatures of obligate symbiosis. BMC Genomics 25: 529. doi:10.1186/s12864-024-10391-2.

Round ER. 2021. {glottoTrees}: Phylogenetic trees in Linguistics. https://github.com/erichround/glottoTrees.

Schliep K, Potts AJ, Morrison DA and Grimm GW. 2017. Intertwining phylogenetic trees and networks. Methods in Ecology and Evolution 8: 1212–1220. doi:10.1111/2041-210X.12760.

Shen X-X, Steenwyk JL and Rokas A. 2021. Dissecting Incongruence between Concatenation- and Quartet-Based Approaches in Phylogenomic Data. Syst Biol 70: 997–1014. doi:10.1093/sysbio/syab011.

Slowikowski K. 2024. ggrepel: Automatically Position Non-Overlapping Text Labels with "ggplot2." https://cran.r-project.org/package=ggrepel.

Smith ML and Hahn MW. 2021. New Approaches for Inferring Phylogenies in the Presence of Paralogs. Trends in Genetics 37: 156–169. doi:10.1016/j.tig.2020.08.012.

Steenkamp ET, Wingfield MJ, McTaggart AR and Wingfield BD. 2018. Fungal species and their boundaries matter – Definitions, mechanisms and practical implications. Fungal Biology Reviews 32: 104–116. doi:10.1016/j.fbr.2017.11.002.

Steensels J, Gallone B and Verstrepen KJ. 2021. Interspecific hybridization as a driver of fungal evolution and adaptation. Nat Rev Microbiol 19: 485–500. doi:10.1038/s41579-021-00537-4.

Steenwyk JL, Li Y, Zhou X, Shen X-X and Rokas A. 2023. Incongruence in the phylogenomics era. Nat Rev Genet 24: 834–850. doi:10.1038/s41576-023-00620-x.

Téllez MD, Batista-Duharte A, Portuondo D, Quinello C, Bonne-Hernández R and Carlos IZ. 2014. *Sporothrix schenckii* complex biology: environment and fungal pathogenicity. Microbiology 160: 2352–2365. doi:10.1099/mic.0.081794-0.

Tralamazza SM, Gluck-Thaler E, Feurtey A and Croll D. 2024. Copy number variation introduced by a massive mobile element facilitates global thermal adaptation in a fungal wheat pathogen. Nat Commun 15: 5728. doi:10.1038/s41467-024-49913-7.

Uehling J, Deveau A and Paoletti M. 2017. Do fungi have an innate immune response? An NLR-based comparison to plant and animal immune systems. PLoS Pathog 13: e1006578. doi:10.1371/journal.ppat.1006578.

Urban M, Cuzick A, Seager J, Nonavinakere N, Sahoo J, Sahu P, Iyer VL, Khamari L, Martinez MC and Hammond-Kosack KE. 2025. PHI-base – the multi-species pathogen–host interaction database in 2025. Nucleic Acids Research 53: D826–D838. doi:10.1093/nar/gkae1084.

Urquhart AS, Chong NF, Yang Y and Idnurm A. 2022. A large transposable element mediates metal resistance in the fungus *Paecilomyces variotii*. Curr Biol 32: 937–950. doi:10.1016/j.cub.2021.12.048.

Urquhart AS, Gluck E and Vogan AA. 2024. Gene acquisition by giant transposons primes eukaryotes for rapid evolution via horizontal gene transfer. Sci. Adv. 10: eadp8738. doi:10.1126/sciadv.adp8738.

Urquhart AS, Vogan AA, Gardiner DM and Idnurm A. 2023. *Starships* are active eukaryotic transposable elements mobilized by a new family of tyrosine recombinases. PNAS 120: e2214521120. doi:10.1073/pnas.2214521120.

Van Etten J, Stephens TG and Bhattacharya D. 2023. A *k*-mer-Based Approach for Phylogenetic Classification of Taxa in Environmental Genomic Data. Syst Biol 72: 1101–1118. doi:10.1093/sysbio/syad037.

VanWallendael A and Alvarez M. 2022. Alignment-free methods for polyploid genomes: Quick and reliable genetic distance estimation. Molecular Ecology Resources 22: 612–622. doi:10.1111/1755-0998.13499.

Větrovský T, Morais D, Kohout P, Lepinay C, Algora C, Awokunle Hollá S, Bahnmann BD, Bílohnědá K, Brabcová V, D'Alò F, *et al.* 2020. GlobalFungi, a global database of fungal occurrences from high-throughput-sequencing metabarcoding studies. Scientific Data 7: 228. doi:10.1038/s41597-020-0567-7.

Vogan AA, Ament-Velásquez SL, Bastiaans E, Wallerman O, Saupe SJ, Suh A and Johannesson H. 2021. The *Enterprise*, a massive transposon carrying *Spok* meiotic drive genes. Genome Res. 31: 789–798. doi:10.1101/gr.267609.120.

Wells JN and Feschotte C. 2020. A Field Guide to Eukaryotic Transposable Elements. Annu Rev Genet 54: 539–561. doi:10.1146/annurev-genet-040620-022145.

Wicker T, Sabot F, Hua-Van A, Bennetzen JL, Capy P, Chalhoub B, Flavell A, Leroy P, Morgante M, Panaud O, *et al.* 2007. A unified classification system for eukaryotic transposable elements. Nat Rev Genet 8: 973–982. doi:10.1038/nrg2165.

Wickham H, Averick M, Bryan J, Chang W, McGowan L, François R, Grolemund G, Hayes A, Henry L, Hester J, *et al.* 2019. Welcome to the Tidyverse. J Open Source Softw 4: 1686. doi:10.21105/joss.01686.

Wickham H and Seidel D. 2023. scales: Scale Functions for Visualization. https://cran.r-project.org/package=scales.

Wilke CO. 2024. cowplot: Streamlined Plot Theme and Plot Annotations for "ggplot2." https://cran.r-project.org/package=cowplot.

Xu S, Dai Z, Guo P, Fu X, Liu S, Zhou L, Tang W, Feng T, Chen M, Zhan L, *et al.* 2021. ggtreeExtra: Compact Visualization of Richly Annotated Phylogenetic Data. Mol Biol Evol 38: 4039–4042. doi:10.1093/molbev/msab166.

Yu G, Smith DK, Zhu H, Guan Y and Lam TT-Y. 2017. GGTREE: an R package for visualization and annotation of phylogenetic trees with their covariates and other associated data. Methods Ecol Evol 8: 28–36. doi:10.1111/2041-210X.12628.

Zielezinski A, Girgis HZ, Bernard G, Leimeister C-A, Tang K, Dencker T, Lau AK, Röhling S, Choi JJ, Waterman MS, *et al.* 2019. Benchmarking of alignment-free sequence comparison methods. Genome Biol 20: 144. doi:10.1186/s13059-019-1755-7.

Zielezinski A, Vinga S, Almeida J and Karlowski WM. 2017. Alignment-free sequence comparison: benefits, applications, and tools. Genome Biol 18: 18–186. doi:10.1186/s13059-017-1319-7.

Table 1. PHI-base genes with BLAST hits in *Gaeumannomyces Starship* cargos. * Pectate lyases CcpelA and PELB matched to the same orthogroup. † *Pyricularia oryzae* = *Magnaporthe oryzae*

PHI-base ID	Gene	Function	Species	Mutant phenotype	Plant host
PHI:7559	FgGT2	glycosyltransferase	*Fusarium graminearum*	loss of pathogenicity	*Triticum aestivum*
PHI:2057	MoPLC1	modulator of calcium flux	*Pyricularia oryzae* †	loss of pathogenicity	*Oryza sativa*
PHI:3837	Sre1	iron-sensitive transcription factor	*Bipolaris maydis*	reduced virulence	*Zea mays*
PHI:2476	CcpelA *	pectate lyase	*Colletotrichum coccodes*	reduced virulence	*Solanum lycopersicum*
PHI:222	PELB *	pectate lyase	*Colletotrichum gloeosporioides*	reduced virulence	*Persea americana*
PHI:9042	nrps5 (FGSG_13878)	non-ribosomal peptide synthetase	*Fusarium graminearum*	reduced virulence	*Triticum aestivum*
PHI:6262	FUG1	role in pathogenicity and fumonisin biosynthesis	*Fusarium verticillioides*	reduced virulence	*Zea mays*
PHI:3315	conx1	Zn^2Cys^6 transcription factors	*Pyricularia oryzae* †	reduced virulence	*Oryza sativa*
PHI:3308	cnf1	Zn^2Cys^6 transcription factors	*Pyricularia oryzae* †	reduced virulence	*Hordeum vulgare*
PHI:2113	Kin4	Ca^{2+}/CAM-dependent serine/threonine protein kinases	*Pyricularia oryzae* †	reduced virulence	*Hordeum vulgare*
PHI:144	CHT42	chitinase	*Trichoderma virens*	reduced virulence	*Rhizoctonia solani*
PHI:3210	FfSge1	morphological switch regulator	*Fusarium fujikuroi*	unaffected pathogenicity	*Oryza sativa*
PHI:1603	GzOB044	transcription factor	*Fusarium graminearum*	unaffected pathogenicity	*Triticum*
PHI:1377	GzC2H040	transcription factor	*Fusarium graminearum*	unaffected pathogenicity	*Triticum*
PHI:6639	Modnm3	dynamin	*Pyricularia oryzae* †	unaffected pathogenicity	*Oryza sativa*
PHI:6613	Mocapn14	calpain	*Pyricularia oryzae* †	unaffected pathogenicity	*Oryza sativa*
PHI:124206	Xyp1 (Uv8b_02447)	cell wall degrading enzymes	*Ustilaginoidea virens*	increased virulence	*Oryza sativa*

Figure 1. Kmer-based phylogenetic analyses of *Starship* elements. a) An unrooted kmer-based phylogenetic tree of 53 *Starships* – 39 curated elements from 33 *Pezizomycotina* species (Gluck-Thaler *et al*. 2022; Gluck-Thaler and Vogan 2024) and 14 predicted by starfish from *Gaeumannomyces* species (Hill *et al*. 2025). Grey branches indicate bootstrap support < 70. Tip points are coloured by genus and the outer ring indicates total element length. Black stars beside tips highlight elements from another genus in an otherwise monophyletic clade. b) A tanglegram comparing the topology of the kmer-based element tree in Fig. 1a and a maximum-likelihood gene tree of the corresponding captain genes (see Supplementary Fig. 1 for the unrooted captain tree). Both trees are arbitrarily rooted with the Msp_Enterprise element. Grey branches indicate bootstrap support < 70. c) An unrooted kmer-based phylogenetic tree of 617 *Starships* predicted with starfish (Gluck-Thaler and Vogan 2024; Hill *et al*. 2025), with grey branches indicating bootstrap support < 70. Genus-level monophyletic clades are highlighted and labelled, with the number of elements in each clade shown in brackets. Clades and tips are coloured by host taxonomic class. See Supplementary Fig. 2 for element tip labels and captain-based family classifications. d) A summary of the kmer-based tree in Fig. 1c with genus-level monophyletic clades collapsed. The outer grid summarises *Starship* family classifications based on captain genes for the elements in each clade, with a darker grid cell colour indicating a higher proportion of the elements within the clade belonging to that family. Clades with no grid cells did not have any classified captain data.

Figure 2. Summary of the *Gaeumannomyces Starships* predicted using starfish by Hill et al. (2025). a) A schematic of the 20 *Starships* ordered by phylogenetic relationships taken from Supplementary Fig. 2. Synteny between orthologous genes in neighbouring elements is indicated with grey lines. A nested element (Ga-3aA1_s00047) is highlighted in yellow. Common genes are coloured with known functions and the presence of flanking direct repeats (DRs) or tandem inverted repeats (TIRs) are indicated with an asterisk. Genes of note are labelled in black boxes. b) Ideograms showing the position of the 20 *Starships* across pseudochromosomes, adapted from Hill et al. (2025). ID numbers correspond to the bolded numbers for each element in Fig. 2a. Elements with flanking DRs are indicated with asterisks either side of the element ID number.

Figure 3. Comparison of cargo gene content similarity across *Gaeumannomyces Starships*. a) An upset plot indicating groups of elements which share at least five orthologous genes (accessory), and elements with at least five unique cargo genes (specific). Elements are ordered by phylogenetic relationships taken from Supplementary Fig. 2. Total number of cargo orthogroups is shown in the

right-hand bar plot with the proportion of accessory and specific cargo genes coloured per element. Element rows are coloured by host lineage. A representation of all shared accessory orthologous genes is given in Supplementary Fig. 7. (b) An upset plot indicating the ratio of orthologous genes shared across lineage/species boundaries. (c) A tanglegram comparing the topology of *Gaeumannomyces* elements taken from Supplementary Fig. 2 and a hierarchical clustering of cargo orthologous gene presence/absence.

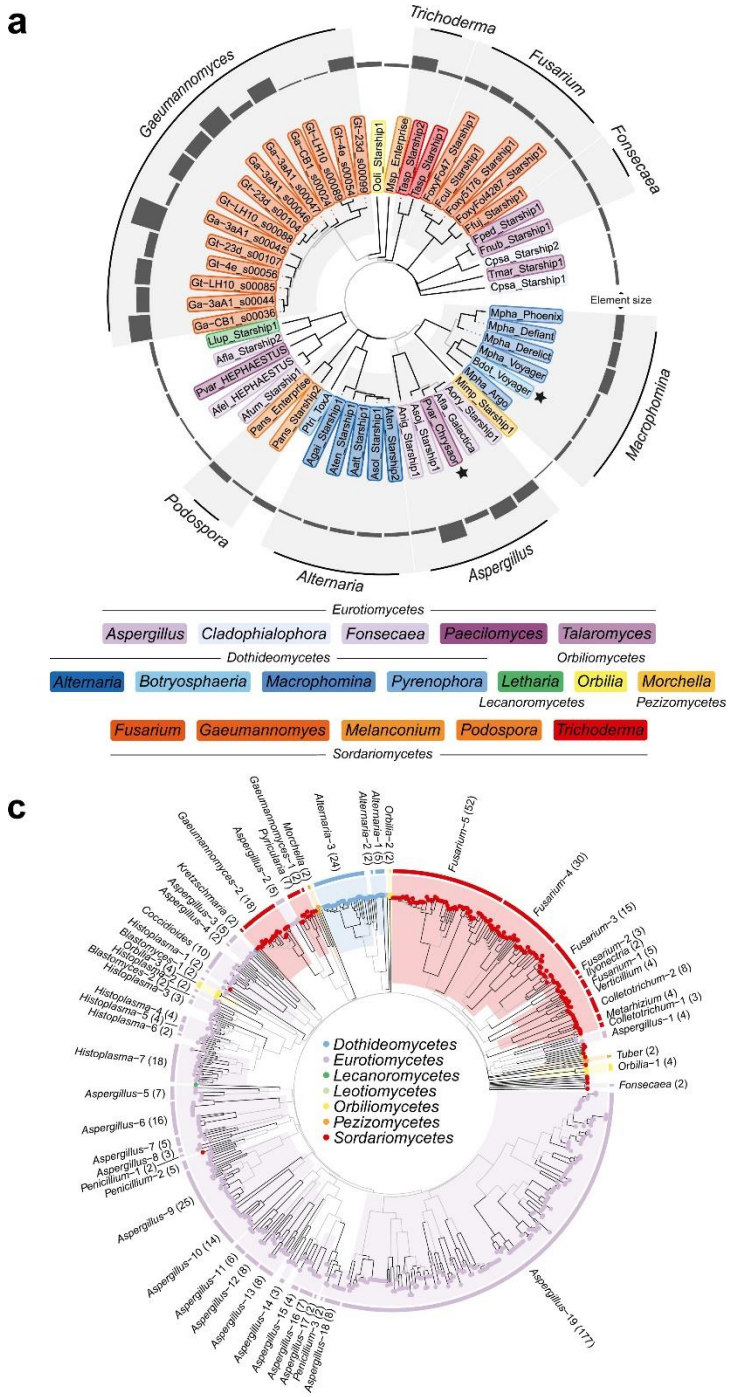

Figure 1
174x184 mm (DPI)

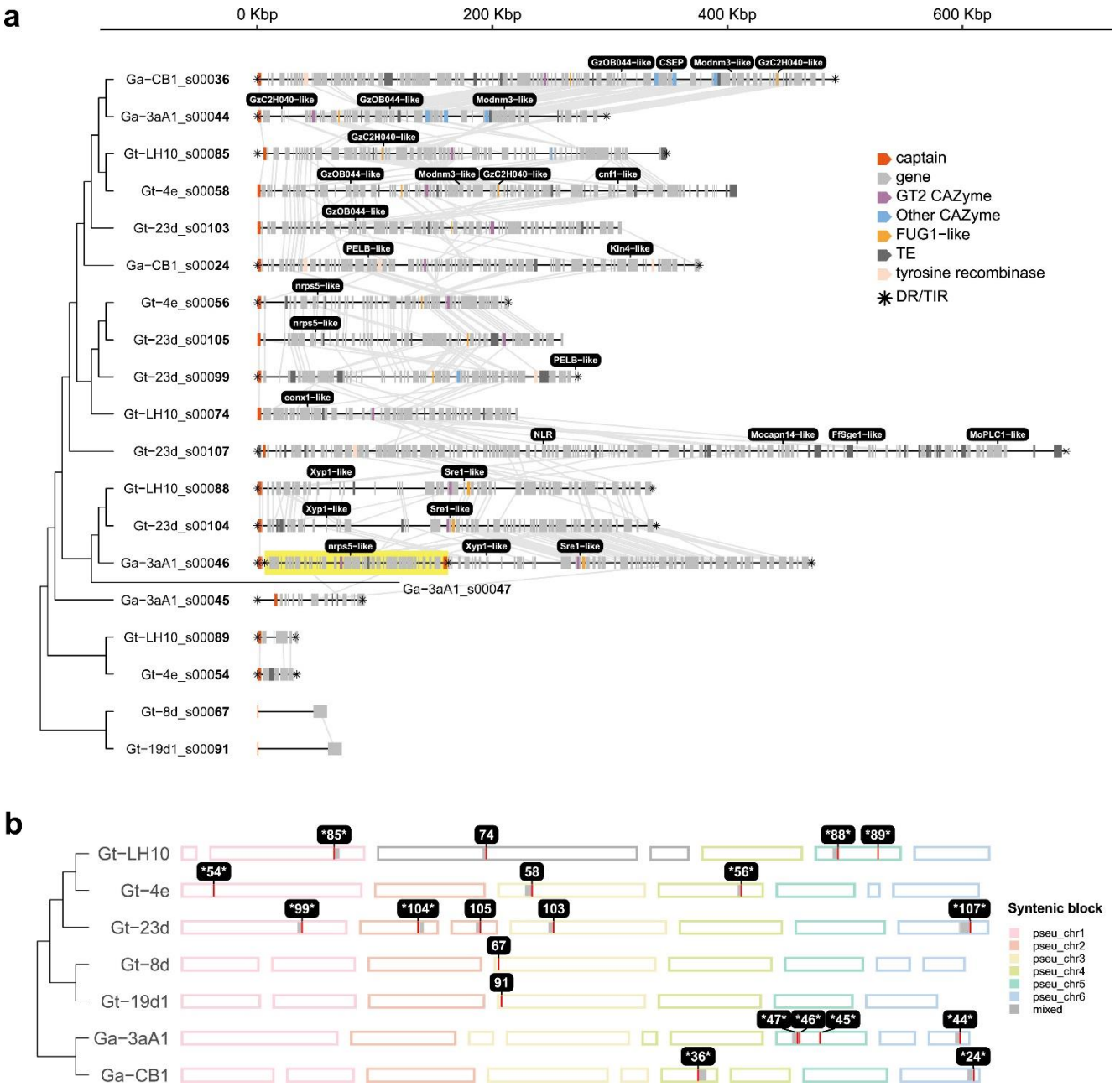

Figure 2
175x169 mm (DPI)

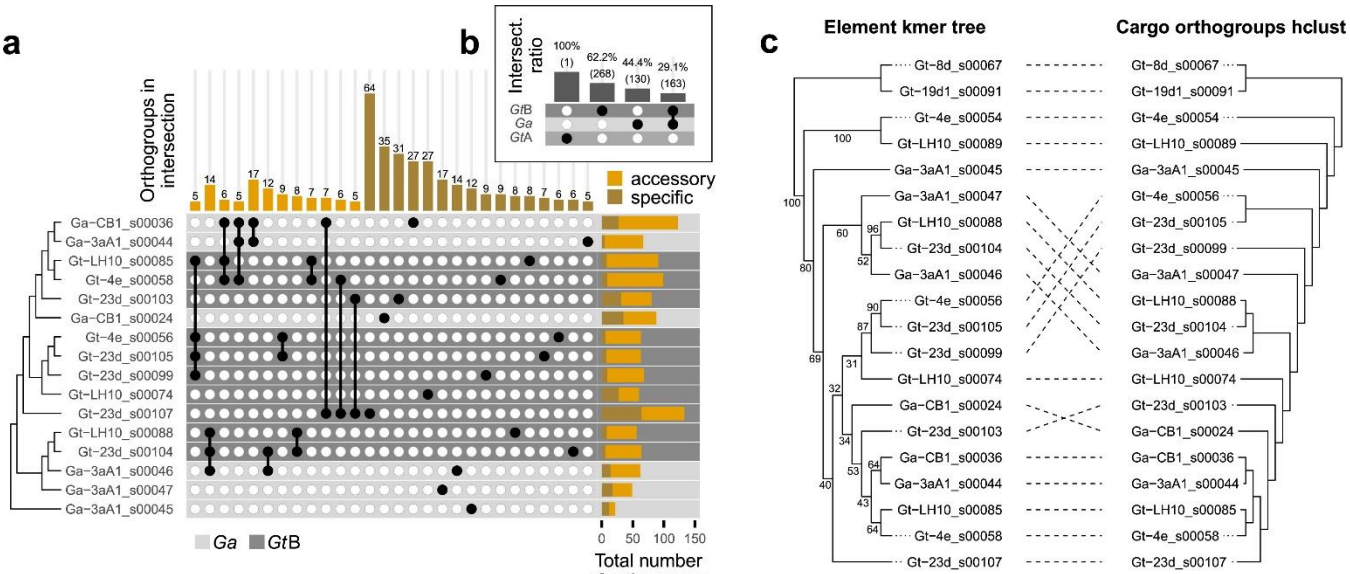

Figure 3
178x78 mm (DPI)

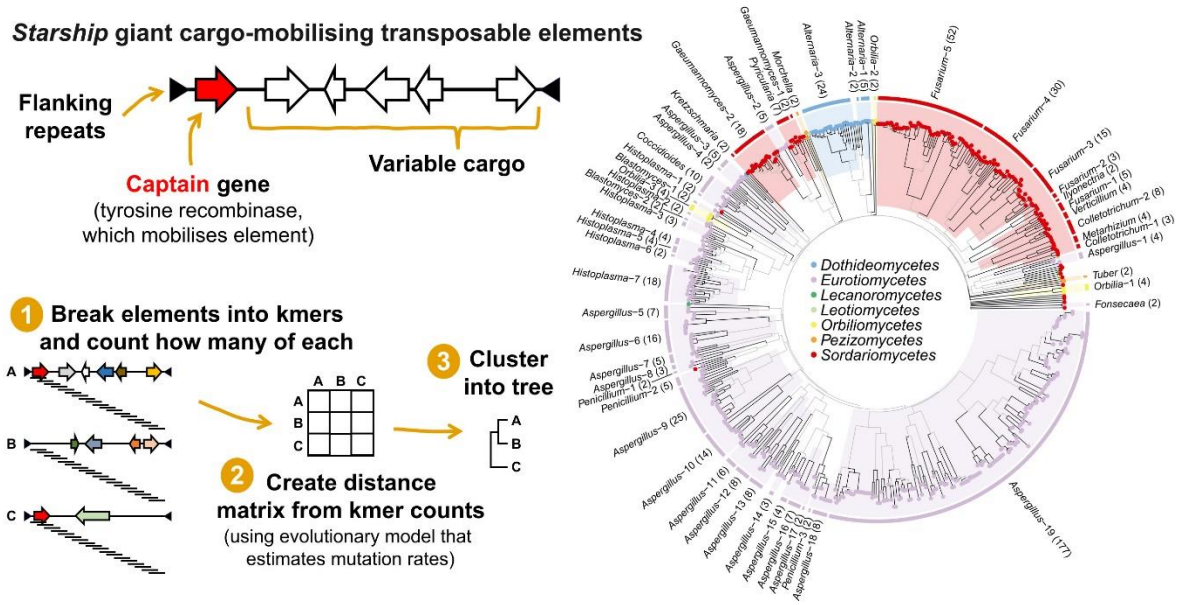

Graphical Abstract